Vibrations of Bladed Disk Assemblies

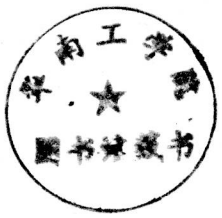

Vibrations of Bladed Disk Assemblies

presented at

THE NINTH BIENNIAL CONFERENCE ON
MECHANICAL VIBRATION AND NOISE
OF THE DESIGN AND PRODUCTION
ENGINEERING TECHNICAL CONFERENCES
DEARBORN, MICHIGAN
SEPTEMBER 11-14, 1983

sponsored by

THE DESIGN ENGINEERING DIVISION, ASME

edited by

D. J. EWINS
IMPERIAL COLLEGE OF SCIENCE
AND TECHNOLOGY
LONDON, ENGLAND

A. V. SRINIVASAN
UNITED TECHNOLOGIES RESEARCH CENTER
EAST HARTFORD, CONNECTICUT

THE AMERICAN SOCIETY OF MECHANICAL ENGINEERS
United Engineering Center 345 East 47th Street New York, N. Y. 10017

Library of Congress Catalog Card Number 83-72174

FOREWORD

In the seven years that have elapsed since the publication of a previous collection of papers on the structural dynamic aspects of bladed disc assemblies (ASME, 1976), there has been continued awareness of the complexity and importance of this topic, Indeed, in the past two or three years, there has been a widespread renewal of research activity on the vibration of bladed assemblies, including not only the structural dynamics but also the aerodynamics aspects as well. Thus it is appropriate at this juncture to bring together a collection of papers into the present volume in order to provide a comprehensive review of the current state of the subject.

A total of 17 papers are included in the volume, covering a wide range of studies most of which are concerned with the particular features of assemblies of blades. They all share one common feature and that is an attempt to prove further into, or to understand better the extremely complex characteristics which are a hallmark of most blade vibration phenomena encountered in practice. It is not appropriate to separate these papers into distinct categories – many of them cover a wide range of aspects – but we may review them in a general way to obtain an overall picture of the main areas of current interest. First, we can identify a number of papers whose main objective is the development of more accurate or more refined analytical methods that seek to provide better predictions of the structural dynamic characteristics of interest – namely, assembly natural frequencies and forced response properties. This group includes the contributions from Lalanne et al, Rao & Jadvani, Ewins & Imregun, Janecki, Chia-Fu Sheng & Mosimann, Crawley & Mokadam. Next there are three papers – by Srinivasan & Cutts, Fu & Zhou and Wachter et al – which provide contributions from a primary experimental standpoint; presenting detailed observations of how particular structural assemblies actually behave in practive. We should never forget that all our analytical predictions are based on *assumptions* of the system's behaviour and that these studies must be verified and, if necessary, modified in the light of actual behaviour. For this process to be effective, advanced and detailed experimental techniques will remain an essential tool for many years to come.

The next two papers – by Halliwell & Lit and Ford & Srinivasan – deal with the necessary process of combining the structural and aerodynamic aspects for an analysis of flutter. In actual operation, almost all blade vibration phenomena necessarily include both of these ingredients and the day is probably not far away when a bladed assembly vibration analysis will automatically incorporate both a complex structural dynamic model and a realistic representation of the conditions which provide both the excitation and the damping effects.

In the last group of papers – six in total, including contributions by Griffin & Hoosac, Irretier, Ewins & Han, Jones & Muszynska, Lu & Warner, and MacBain & Whaley – all describe studies which have been made of the problem of mistuning. This very real practical problem of how closely tuned should the set of blades be in any one assembly is now reveiving considerable attention. It is widely accepted that mistuning is generally undesirable from the point of view of forced response levels but, conversely, is advantageous in respect of flutter. Most of the papers included here address the first of these problems and seek an answer to the perennial question: "How should a given set of blades be arranged so as to minimize the detrimental effects of mistuning?" A definite answer is not yet available but probably will be by the time the next of these volumes in produced.

The preparation of such a volume as this is only possible through the contributions and cooperation of the authors and the reviewers all of which are gratefully acknowledged. In particular, the extra efforts made in order to meet the final deadlines were much appreciated. We hope, on their and our own behalf, that the contents of this volume have something to offer all those whose interests include the study of blade and disc vibration.

D. J. Ewins, London, England
A. V. Srinivasan, East Hartford, Connecticut, USA

CONTENTS

FREQUENCIES AND MODE SHAPES OF ROTATING BLADED AXISYMMETRIC STRUCTURES. APPLICATION TO A JET ENGINE

G. Ferraris, Ingenieur de Recherche, **R. Henry,** Maitre-Assistant, **M. Lalanne,** Professeur,
P. Trompette, Professeur
Laboratoire de Mecanique des Structures, E. R. A. C. N.R.S. 911
Institute National des Sciences Appliques
Villeurbanne, France

SUMMARY

This paper deals with the prediction of the dynamic behaviour of bladed axisymmetric systems. The structure consists of axisymmetric components having thin and thick parts and a high number of twisted blades. The thin parts are modeled with thin shell axisymmetric elements, the thick parts with thick isoparametric elements and the blades with twisted beam elements, including predominant effects such as bending bending and bending-torsion coupling. Junction elements are used to insure slope and displacement continuity between the various finite elements having three, four and six degrees of freedom per node. Kinetic and strain energies, including the rotating effects are calculated and governing equations are derived using Lagrange's equations. The developed method and the associated computer program is applied to the determination of frequencies and mode shapes of a rotating low pressure stage of a recent jet engine.

NOMENCLATURE

A	coefficient matrix
C	shear center of a cross section
E	Young's modulus
F,f	force and generalized force vector
G	centroid of a cross section
$G\ J_T$	torsional rigidity
K,k	stiffness and generalized stiffness matrices
L	finite element length
M,m	mass and generalized mass matrices
$M_1,M_2,\ldots$	typical points
$N_1,N_2,\ldots$	displacement functions matrices
N	blade number
NI,NJ	finite element nodes
n	nodal diameter number
$R(G x\xi\eta)$	local coordinate system
$R_O(OXYZ)$	global coordinate system
S	blade typical cross section
T,U	kinetic and strain energies
V_M	typical point absolute velocity
u_x,u_y,u_z,u,v,w	typical point displacements
ϕ_ξ,ϕ_η,ϕ	bending slopes and torsion angle in cartesian systems
u_r,u_z,u_θ,ψ	typical point displacements and slope in axisymmetric systems
x,y,z,s,ξ,η	cartesian coordinates
r,z,θ	axisymmetric coordinates
V	volume
δ	finite element nodal displacements
δ_1,δ_2	generalized displacements
θ'	rate of pretwist
ξ_I,η_I,x_I	components of $\overrightarrow{OG_I}$ in R coordinate system
ξ_t,η_t	shear center coordinates in R
$\bar{f}$	dimensionless frequency
ρ	mass per unit volume
σ_0	initial stress
$\varepsilon,\varepsilon_\ell,\varepsilon_{n\ell}$	longitudinal strains
$\Omega(\Omega_1,\Omega_2,\Omega_3)$	angular velocity and its components in the R system
$\bar{\Omega}$	dimensionless speed of rotation
ω	pulsation rd/s

Superscripts

$\{\ \}^t,\ \|\ \|^t$	denotes transpose of a matrix
$\dot{(\ )}$	time first derivation (velocity)
$\ddot{(\ )}$	time second derivation (acceleration)
$(\ )'$	x first derivative
$(\ )''$	x second derivative
$*$	free vibration
$\rightarrow$	arrow denotes a vector quantity

Subscripts

O	related to a single blade or n = O nodal diameter
c	denotes centrifugal effect
e	related to a typical finite element
F	denotes bending effect
G	related to centroïd
g	denotes non linear geometric effect
i,j	related to typical sections S_i,S_j
M	related to a typical point M
T	denotes torsion effect
$\lvert\overrightarrow{M_1M_2}\rvert$	modulus of the vector $\overrightarrow{M_1M_2}$

INTRODUCTION

In turbomachinery, the rotating elements such as the bladed disc assemblies, are the most critical parts of the design. Thus, the manufacturers are interested in any improvements in dynamic analysis methods. We are concerned here with the prediction of frequencies and mode shapes of jet engine turbine stages.

Several investigators Armstrong |1|, Ewins |2|, |3|, Cottney |4| and Kirkhope-Wilson |5|, have studied the vibration characteristics of thin bladed-disc assemblies.

In their approach, the disc is a circular plate and rectangular cross section beam elements represent the blading. In |6|, Thomas has included the effect of an asymmetric pretwisted cross-section blade. The prediction of the dynamic behaviour of axisymmetric structures is now well known |7|, |8|. On the otherhand, many papers have been written on the vibration of rotating beams and blades along with review articles by J.S. Rao |9|, |10|, |11| and Leissa |12|, |13|.

In |1-6 |the bladed disc systems have an axisymmetric behaviour characterized by diametral and circular nodal lines. This hypothesis is confirmed by experiment, and is valid for structures having a large number of blades mounted on a disc and for a large range of modes. As a consequence, the modelisation can be achieved on a much simpler way because the required number of degrees of freedom is small. When the mode shapes are not axisymmetric, methods using cyclic symmetry can be introduced |14|, |15|, |16| ; thus impellers are excluded from consideration.

For the typical axisymmetric bladed structures considered here, experiments have shown that their dynamic behaviour still has axisymmetric characteristics.

As shown in figure 1, these structures consist of :

- axisymmetric cylindrical components having thin and thick parts without plane of symmetry.
- high number of blades modeled as beams where bending-bending and bending-torsion effects are taken into account.

In this paper, the application presented is a rotating low pressure turbine stage of a recent jet engine. The finite element method, very well suited for complex structures, is used. Strain and kinetic energies of the various elements are determined, then the finite elements are introduced in the calculations and the Lagrange equations applied. The natural frequencies and associated mode shapes are obtained by solving an eigenvalue-eigenvector problem.

An inertial reference axis system is used such that X is directed radially outwards, Y is directed tangentially, and Z is directed parallel to the axis of rotation. The structure is rotating at a constant angular velocity Ω. The material is assumed to be homogeneous and linear elastic, and natural vibrations are assumed to be of small amplitude.

AXISYMMETRIC STRUCTURE MODELISATION

The turbine stage presented in figure 1 shows an axisymmetric component which has thin and thick parts ; thus, at least two types of finite element are needed - thin shell and thick axisymmetric elements. The thin shell element used here has 2 nodes and 4 degrees of freedom (DOF) per node and the thick isoparametric element has 8 nodes and 3 DOF per node. These two elements are classical and will be briefly presented. Continuity between 3 DOF per node elements and 4 DOF per node elements is ensured by massless special thin

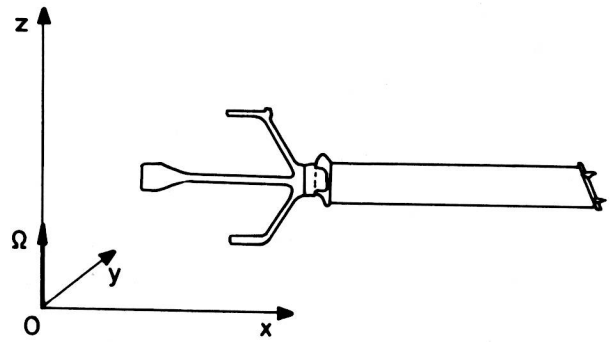

Fig.1 : Simplified representation of a jet engine turbine stage (low pressure).

shell elements called "junction elements" whose thickness and Young's modulus values are derived from mechanical considerations detailed and checked in |18|, and used in |17|.

Thin axisymmetric element. Figure 2 shows this element, the thickness is constant and displacements are expressed in term of trigonometric series as follows :

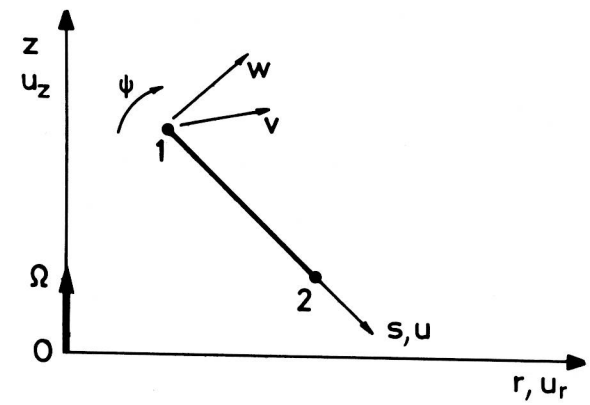

Fig.2 : Thin shell axisymmetric element.

$$u = \sum_n u_n \cos n\theta$$
$$v = \sum_n v_n \sin n\theta \qquad (1)$$
$$w = \sum_n w_n \cos n\theta$$

The displacement functions and the four nodal degrees of freedom are :

$$u_n = a_1 + a_2 s$$
$$v_n = a_3 + a_4 s \qquad (2)$$
$$w_n = a_5 + a_6 s + a_7 s^2 + a_8 s^3$$

and

$$\{\delta\} = \{u_{rn},\ u_{zn},\ u_{\theta n},\ \psi_n = -\frac{\partial w_n}{\partial s}\}^t \qquad (3)$$

Strain displacement relations, including non linear effects due to rotation are found in Novozhilov thin shell theory |19|.

Thick isoparametric element. Figure 3 shows this element. The displacements are expressed by :

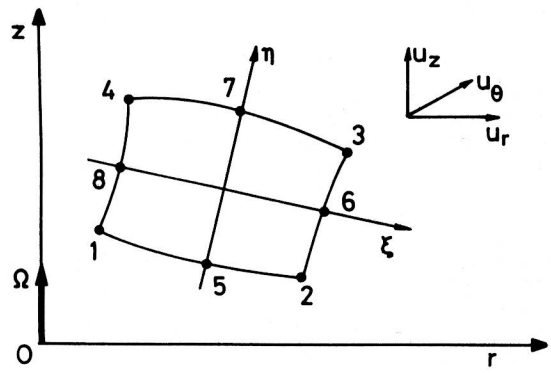

Fig.3 : Thick isoparametric axisymmetric element.

$$
\begin{aligned}
u_r &= \Sigma\, u_{rn} \cos n\theta \\
u_z &= \Sigma\, u_{zn} \cos n\theta \\
u_\theta &= \Sigma\, u_{\theta n} \sin n\theta
\end{aligned}
\qquad (4)
$$

with

$$
u_{rn} = \sum_{i=1}^{8} N_i\, u_{rni}
$$

$$
u_{zn} = \sum_{i=1}^{8} N_i\, u_{zni} \qquad (5)
$$

$$
u_{\theta n} = \sum_{i=1}^{8} N_i\, u_{\theta ni}
$$

and

$$
\begin{aligned}
N_1 &= -\frac{1}{4}(1-\xi)(1-\eta)(1+\xi+\eta) \\
N_2 &= -\frac{1}{4}(1+\xi)(1-\eta)(1-\xi+\eta) \\
N_3 &= -\frac{1}{4}(1+\xi)(1+\eta)(1-\xi-\eta) \\
N_4 &= -\frac{1}{4}(1-\xi)(1+\eta)(1+\xi-\eta) \\
N_5 &= \frac{1}{2}(1-\xi^2)(1-\eta) \\
N_6 &= \frac{1}{2}(1+\xi)(1-\eta^2) \\
N_7 &= \frac{1}{2}(1-\xi^2)(1+\eta) \\
N_8 &= \frac{1}{2}(1-\xi)(1-\eta^2)
\end{aligned}
\qquad (6)
$$

the three nodal DOF are :

$$
\delta = \{u_{rn},\ u_{zn},\ u_{\theta n}\}^t \qquad (7)
$$

Strain displacement relations including geometric non linear effects are given in |20|.

Junction element. As the thick isoparametric element has three degrees of freedom per node and the thin shell element four DOF per node, the connection between thick and thin parts of the structure must be treated with care.

The aim of a junction element is to ensure the continuity of the slope ψ. This is achieved by plating (fig.4) two thin shell elements I, II between thick element nodes 1, 2, 3 and the first thin shell element III.

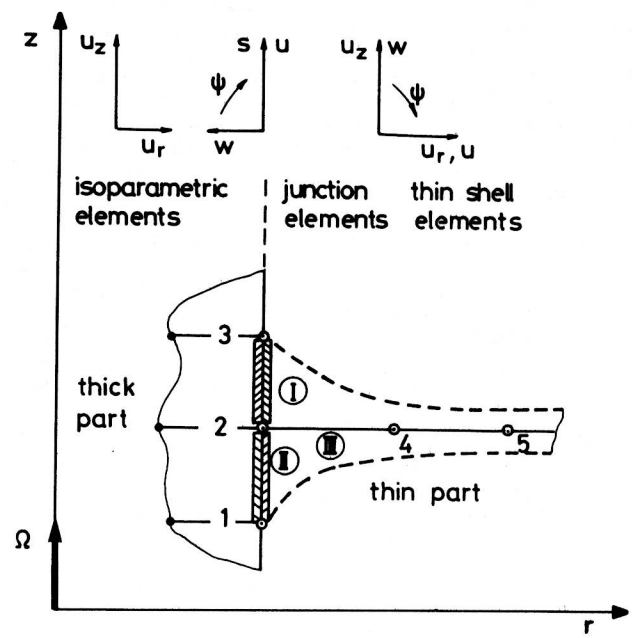

Fig.4 : Junction elements.

Thus, displacement continuity is achieved. The adequate hardening of the slope stiffness terms of the junction elements is guaranted by the rigid rotation displacements of the facets (1-2 and 2-3). Practically, finite elements I and II are defined with the thickness of element III in which displacement stiffness terms are divided by 100 and slope stiffness terms multiplied by the same number. To avoid perturbation in dynamic behaviour, mass per unit volume ρ is taken as zero. This element has been detailed and checked in |17| and |18|.

BLADING MODELISATION

If it is assumed that the number, N, of blades is large, and that the system vibrates at a small number, n, of nodal diameters, the blades can be considered to be continuously distributed on the rim around the axisymmetric structure. Thus, following |1|, the blade array strain and kinetic energies U, T, may be obtained from the strain and kinetic energies of a single blade U_o, T_o. These are

$$
U = \frac{N}{2} U_o \quad , \quad T = \frac{N}{2} T_o \qquad (8)
$$

For the symmetric case, i.e. when the number of nodal diameters n = 0, the coefficient 1/2 has to be canceled. Thus, noting that U_o and T_o are independent of n, the stiffness and mass matrices of the vibrating array of blades are those of a single blade weighted by the factor N or N/2 according to the value of n.

This part of the paper is devoted to the derivation of a beam finite element suitable for jet engine turbine blade modelisation.

In general, a turbine blade is pretwisted : it has an asymmetrical varying aerofoil cross section and is mounted with a stagger angle. Depending on the geometrical characteristics, the turbine blading can execute either uncoupled bending or torsional vibrations or coupled bending-torsion vibrations. Coupled bending-torsion vibrations occur when the shear center does not

coincide with the centroid of the blade cross section. When the blade is pretwisted, vibrations in rotation are further coupled between the two bending modes. In addition, coupling exists between longitudinal and torsional motions (untwist due to centrifugal effects) and between longitudinal constraints and bending (centrifugal stiffening). The finite element presented takes into account these fundamental effects. Strain energy U is calculated as the sum of energy (U_F) due to extension of a fiber and shear energy (U_T) due to torsion. Derivation of U_T is straight forward but that of U_F has to be more detailed. U_F is expressed in term of the longitudinal strain ε defined as the ratio between the fiber length difference after and before extension, and its undeformed length. ε is then found to contain linear and non linear terms needed to describe the effects mentioned previously. Kinetic energy is derived from the calculation of the velocity of a typical point expressed in a coordinate system linked to the rotating structure. As turbine blades are almost radial, Coriolis effects can be neglected [18].

Longitudinal strain determination

On a typical cross section of a blade segment (fig.5) a coordinate system R is located at the centroid G of the section. G_ξ and G_η are the principal inertia axis and G_x is the centroid line. $C(\xi_t,\eta_t)$ is the shear center and $M(\xi,\eta)$ is a typical point of the cross section.

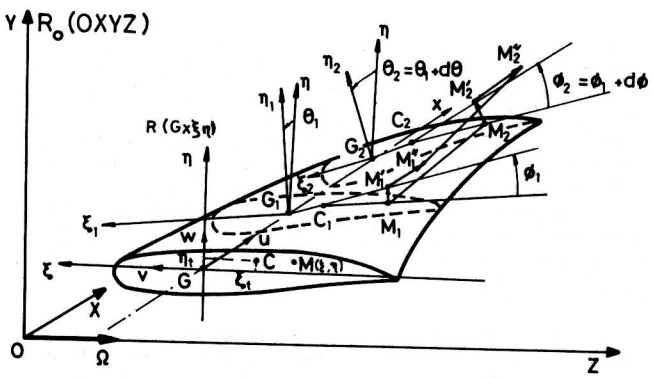

Fig.5 : Main definitions on a twisted blade segment.

Considering section 1 located at x and section 2 at x + dx, one defines respectively for these 2 cross sections : the centroids G1 and G2, the shear centers $C_1(\xi_{t1},\eta_{t1})$ and $C_2(\xi_{t2},\eta_{t2})$, local coordinate systems $G_1\xi_1\eta_1$ and $G_2\xi_2\eta_2$ linked to minimum and maximum second moments of area, the pretwist angles θ_1 and θ_2 with the rate of pretwist $\theta' = d\theta/dx$ and two homologous typical points $M_1(\xi_1,\eta_1)$ and $M_2(\xi_2,\eta_2)$.

Before any deformation, $|\overrightarrow{M_1M_2}|$ is the length of a typical fiber. Following Euler-Bernoulli assumptions, the sections remain plane when deformation occurs. Thus M_1 goes to M'_1 after torsional displacement ϕ_1 and to M''_1 after longitudinal and bending displacements (u,v,w) M_2 goes to M'_2 after torsional displacement $\phi_2 = \phi_1 + d\phi$ and to M''_2 after longitudinal and bending displacements.

Extension of $\overrightarrow{M_1M_2}$ results in $\overrightarrow{M''_1M''_2}$, and the longitudinal strain is defined as :

$$\varepsilon = \frac{|\overrightarrow{M''_1M''_2}| - |\overrightarrow{M_1M_2}|}{|\overrightarrow{M_1M_2}|} \qquad (9)$$

where,

$$\overrightarrow{M_1M_2} = \overrightarrow{M_1G_1} + \overrightarrow{G_1G_2} + \overrightarrow{G_2M_2} \qquad (10)$$

and,

$$\overrightarrow{M''_1M''_2} = \overrightarrow{M''_1M'_1} + \overrightarrow{M'_1C_1} + \overrightarrow{C_1M_1} + \overrightarrow{M_1M_2} + \overrightarrow{M_2C_2} + \overrightarrow{C_2M'_2} + \overrightarrow{M'_2M''_2} \qquad (11)$$

The previous vectors (10), (11) expressed in R(Gx$\xi\eta$) coordinate system and inserted in (9) yield to the expression of the longitudinal strain where ε_ℓ and $\varepsilon_{n\ell}$ represent linear and non linear terms respectively.

$$\varepsilon = \varepsilon_\ell + \varepsilon_{n\ell} \qquad (12)$$

Remembering the small displacement hypothesis and assuming that the chord and the rate of pretwist have a smooth variation along the blade, terms of the form $dx\sqrt{1+a^2}$ are equivalent to $dx(1+a^2/2)$ and $(\xi^2+\eta^2)\theta'^2$ can be neglected in the denominator of Eq.9.

Using notations $|u,v,w,\phi,\theta|' = d/dx\,|u,v,w,\phi,\theta|$ and $|u,v,w|'' = d^2/dx^2|u,v,w|$ and ξ'_t, η'_t being the variation of the shear center position between cross sections 1 and 2, it comes

$$\varepsilon_\ell = u' - \xi v'' - \eta w'' + k\theta'\phi' \qquad (13)$$

$$\varepsilon_{n\ell} = \frac{u'^2}{2} + \xi^2\frac{v''^2}{2} + \eta^2\frac{w''^2}{2} + h\,\phi'^2 + \phi'|(\eta-\eta_t)v'' - (\xi-\xi_t)w''|x + (1+\eta^2\theta'^2)\frac{v'^2}{2} + (1+\xi^2\theta'^2)\frac{w'^2}{2} \qquad (14)$$

$$- \xi\eta\theta'^2 v'w' - \xi\theta'u'w' + \eta\theta'u'v' - \eta u'w'' - \xi u'v'' + \xi\eta v''w'' + \xi^2\theta'v''w' - \eta^2\theta'v'w'' + \xi\eta\theta'w'w'' - \xi\eta\theta'v'v''$$

where

$$k = \eta A - \xi B \quad , \quad h = \frac{A^2+B^2}{2} + \theta'(\xi D - \eta C) \qquad (15)$$

and

$$\begin{aligned} A &= x|(\xi-\xi_t)\theta' - \eta'_t| + (\eta-\eta_t) \\ B &= x|(\eta-\eta_t)\theta' + \xi'_t| - (\xi-\xi_t) \\ C &= \frac{x^2}{2}|(\eta-\eta_t)\theta' + \xi'_t| - x(\xi-\xi_t) \\ D &= \frac{x^2}{2}|-(\xi-\xi_t)\theta' + \eta'_t| - x(\eta-\eta_t) \end{aligned} \qquad (16)$$

Finite element

The finite element proposed is a straight beam element with 2 nodes NI and NJ situated at the cross section centroid ; NI in G_i and NJ in G_j respectively, (fig.6). The element is calculated in a local coordinate system $R_i(G_i x\xi\eta)$ - x axis is colinear to NI - NJ and $G_i\xi$, $G_i\eta$, are the principal inertia axis of the cross section S_i. At each node the displacement vector has 6 components : the longitudinal and bending displacements u,v,w, the torsional displacement ϕ and the bending slopes ϕ_ξ and ϕ_η, defined in (17)

$$\phi_\xi = -w' \quad , \quad \phi_\eta = v' \qquad (17)$$

On matrix form, the element displacement vector is then

$$\delta_e = |u_i, v_i, w_i, \phi_i, \phi_{\xi i}, \phi_{\eta i}, u_j, v_j, w_j, \phi_j, \phi_{\xi j}, \phi_{\eta j}|^t \qquad (18)$$

Assuming linear polynomial expansions for u, ϕ and cubic for v, w

$$\begin{aligned} u &= a_1 + a_2x \\ v &= a_3 + a_4x + a_5x^2 + a_6x^3 \\ w &= a_7 + a_8x + a_9x^2 + a_{10}x^3 \\ \phi &= b_1 + b_2x \end{aligned} \qquad (19)$$

the coefficient matrix A of equation (20) is obtained from (19)

$$|a_1,\ a_2,\ a_3,\ \ldots,\ a_{10},\ b_1,\ b_2|^t = |A|\ \{\delta_e\} \qquad (20)$$

and given in appendix. The strain and kinetic energies for an element can then be derived.

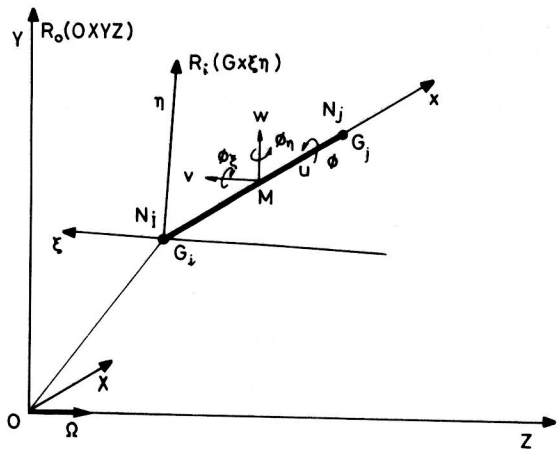

Fig.6 : Twisted beam finite element for the blade.

Element strain energy

The strain energy of an element is the sum of energies due to the longitudinal strain effects U_F and that of torsion U_T.

One has

$$U_e = U_F + U_T \qquad (21)$$

where

$$U_T = \frac{1}{2} G J_T \phi'^2 \qquad (22)$$

G, shear modulus and J_T, torsional constant calculated in |17| from the profile known by point, the other energy component is

$$U_F = \frac{1}{2}\int_V \varepsilon^t E\, \varepsilon\, dV \qquad (23)$$

Where ε is the longitudinal strain given by (12-16), E is Young's modulus and V volume of the element.

Taking $\{\delta_1\}$ as generalized displacement vector

$$\{\delta_1\} = |u',v',w',v'',w'',\phi'|^t \qquad (24)$$

and using (19) and (20) yield

$$\{\delta_1\} = |N_1|\ |A|\ \{\delta_e\} \qquad (25)$$

Element strain energy is derived by substituting equations (12-16) and (19) expressed in term of (25) in (21-23) and integrating over the volume as explained below.

Finally

$$U_e = \frac{1}{2}\{\delta_e\}^t.|K_e + K_g|\ \{\delta_e\} \qquad (26)$$

with

$$|K_e+K_g| = |A|^t \{\int_0^\ell |N_1|^t |k_e+k_g||N_1|\ dx\}|A| \qquad (27)$$

Where matrix $|k_e+k_g|$ is given in the appendix. K_e is the elastic stiffness matrix and K_g the geometric stiffness matrix due to non linear rotating effects.

Element kinetic energy

By definition

$$T_e = \frac{1}{2}\int_V V_M^2\ \rho\ dV \qquad (28)$$

where, ρ is the material mass per unit volume, V_M the velocity of a typical point M expressed by its components in the local rotating system R, (fig.6). The blade rotates at constant angular velocity $\vec{\Omega}$. Its components in R are $(\Omega_1,\Omega_2,\Omega_3)$ and that of $\overrightarrow{OG}$ (x_G,ξ_G,η_G). Calculating $\vec{V}_M$ gives

$$\vec{V}_M = \begin{vmatrix} \dot{u}-\eta\dot{w}'-\xi\dot{v}'+\Omega_2|\eta_G+\eta+w+(\xi-\xi_t)\phi|-\Omega_3|\xi_G+\xi+v-(\eta-\eta_t)\phi| \\ \dot{v}-(\eta-\eta_t)\dot{\phi}-\Omega_1|\eta_G+\eta+w+(\xi-\xi_t)\phi|+\Omega_3|x_G+x+u-\eta w'-\xi v'| \\ \dot{w}+(\xi-\xi_t)\dot{\phi}+\Omega_1|\xi_G+\xi+v-(\eta-\eta_t)\phi|-\Omega_2|x_G+x+u-\eta w'-\xi v'| \end{vmatrix} \qquad (29)$$

Taking $\{\delta_2\}$ as generalized displacement vector

$$\{\delta_2\} = |u,v,w,v',w',\phi|^t \qquad (30)$$

and using (19) and (20) yield

$$\{\delta_2\} = |N_2|\ |A|\ \{\delta_e\} \qquad (31)$$

or

$$\{\dot{\delta}_2\} = |N_2|\ |A|\ \{\dot{\delta}_e\} \qquad (32)$$

The kinetic energy for an element is derived by substituting equation (29) and (19) which are expressed in terms of (31), (32) in (28), and integrating over the volume.

Then it comes

$$T_e = \frac{1}{2}\{\dot{\delta}_e\}^t|M_e|\{\dot{\delta}_e\}+\frac{1}{2}\{\delta_e\}^t|K_c|\{\delta_e\}+\{F_c\}^t\{\delta_e\}+T_c+T_R \qquad (33)$$

with the mass matrix

$$|M_e| = |A|^t \{\rho\int_0^\ell |N_2|^t|m_e||N_2|dx\}\ |A| \qquad (34)$$

the centrifugal stiffness due to mass in rotation

$$|K_c| = |A|^t \{\rho\int_0^\ell |N_2|^t|k_c||N_2|\ dx\}\ |A| \qquad (35)$$

and nodal force vector equivalent to centrifugal forces

$$\{F_c\}^t = \{\rho\int_0^\ell \{f_c\}^t|N_2|\ dx\}\ |A| \qquad (36)$$

Where $|m_e|$, $|k_c|$, $|f_c|$ are given in appendix. T_c, kinetic energy due to Coriolis effects is neglected and T_R does not give any contribution when Lagrange's equations are applied.

Integration procedure

Integration over the volume of an element is performed in two steps. In the first step, integration is done over the element section S, in the second step integration is achieved along the length of the element from node NI to node NJ.

The blade profiles are usually defined by points, thus the surface integrals of the form $\iint_S f(\xi,\eta)d\xi d\eta$ are numerically performed using integral equations technique. For the node sections (NI,NJ) located at x_i and x_j, the first step gives their geometric characteristics i.e. Area, second moments of inertia, shear center coordinates, torsion constant J_T, etc ..., |24|.

As noted earlier, chord and pretwist have smooth variation along the blade, the second integration step

is performed assuming linear variations of the section geometric characteristics with x within the element.

GOVERNING EQUATIONS - FREQUENCIES AND MODE SHAPES

The structure is modeled with the various elements previously presented. The continuity between blades and the axisymmetric structure is ensured for slopes and displacements |17|.

After assembly one gets, for n = O

$$M_o \ddot{\delta}_0 + |K_o + K_{Go}(\sigma_0) - K_{co}|\delta_0 = F(\Omega^2) \qquad (37)$$

and for n ≠ O

$$M_n \ddot{\delta}_n + |K_n + K_{Gn}(\sigma_0) - K_{cn}|\delta_n = O \qquad (38)$$

with M_o, M_n, K_o, K_n, classical mass and stiffness matrices,
K_{Go}, K_{Gn}, geometric stiffness matrices,
K_{co}, K_{cn}, centrifugal stiffness,
$F(\Omega^2)$ and σ_0 respectively the centrifugal force vector and the initial stress distribution.

The solution of system (37) can be written as

$$\delta_0 = \delta_{01} + \delta_{02} \qquad (39)$$

δ_{01}, static displacement vector is obtained in solving

$$|K_o + K_{Go}(\sigma_0) - K_{co}|\delta_{01} = F(\Omega^2) \qquad (40)$$

the stress distribution σ_0 and displacements δ_{01} are unknown initially and are obtained by using a Newton-Raphson procedure.

δ_{02}, the dynamic displacement vector is solution of

$$M_o \ddot{\delta}_{02} + |K_o + K_{Go}(\sigma_0) - K_{co}|\delta_{02} = O \qquad (41)$$

and has the form

$$\delta_{02} = \delta^*_{02} e^{j\omega t} \qquad (42)$$

this gives a classical eigenvalue-eigenvector problem

$$\omega^2 M_o \delta^*_{02} = |K_o + K_{Go}(\sigma_0) - K_{co}|\delta^*_{02} \qquad (43)$$

For n ≠ O, σ_0 is still valuable for K_{Gn} calculation and eq.(38) leads to

$$\omega^2 M_n \delta^*_n = |K_n + K_{Gn}(\sigma_0) - K_{cn}|\delta^*_n \qquad (44)$$

which has to be solved for n = 1,2,3,...

The eigenvalue-eigenvector problems (43) and (44) are solved using a simultaneous iterative method.

APPLICATION TO A LOW PRESSURE TURBINE STAGE

The method presented in this paper has been programed in FORTRAN IV on a VAX 11/780 computer and checked on various test structures. Preliminary tests were performed, and frequencies compared to analytical, numerical and/or experimental results i.e. : a twisted beam |21|, a steam turbine blade |22|, a fan blade and a low pressure turbine blade of a jet engine |17|, axisymmetric plates |23| and a bladed disc assembly |5|. The method is now applied to a rotating low pressure turbine stage of a recent jet engine.

Fig.7 shows the finite element mesh used to calculate frequencies and mode shapes of the above mentioned turbine stage. The disc is mainly modeled with thin shell axisymmetric elements connected to the disc rim using junction elements (I to VI). The rim is modeled with thick isoparametric elements. The blade is modeled with twisted beam elements and continuity of displacements and slopes at the blade root is ensured

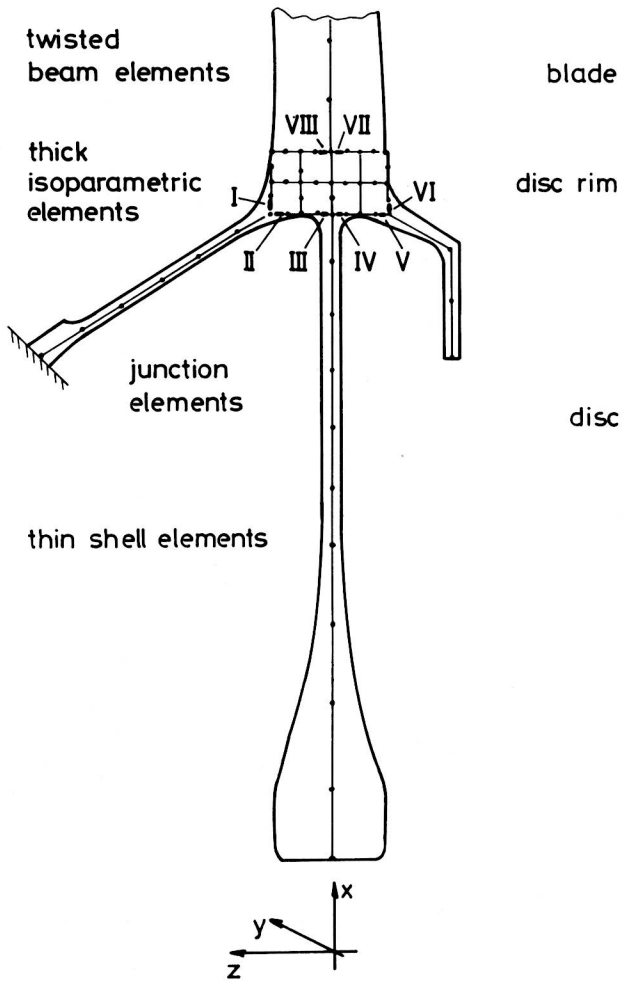

Fig.7 : Low pressure turbine stage. Finite element modelisation.

using two junction elements (VII,VIII) plated on the disc rim. The disc is clamped as shown in fig.7. The blade tip is free in the X and Z directions, supported in Y and retained in torsion.

The frequencies and mode shapes are computed for the structure vibrating with O to 5 nodal diameters at various speeds of rotation Ω. One notes, $\bar{f} = f/f_{01}$ the dimensionless frequency, f_{01} the fundamental frequency at O nodal diameter and $\bar{\Omega} = \Omega/f_{01}$ the dimensionless speed of rotation. The frequencies related to n and $\bar{\Omega}$ are presented in fig.8 and 9. The associated mode shapes are arranged in families f_{nI}, f_{nII}, ..., f_{nVI} and presented in fig.10 to 14.

Family f_{nI}, fig.10, is mainly a disc-rim vibration mode. The blade moves in the XZ plane following the rim motion. It has been verified that the frequency f_{nI} approaches the first bending frequency of the clamped blade for increasing values of nodal diameters. Otherwise, the rotation effects results in a 30 to 40 % increase of the frequencies, (fig.8 and 9).

Family f_{nII}, fig.11, shows a disc bending mode. Rim vibration is limited and the blade bends in the XZ plane. It can be seen in fig.9 that the rotation effect is noticeable on the various n diameters modes (f_{oII},

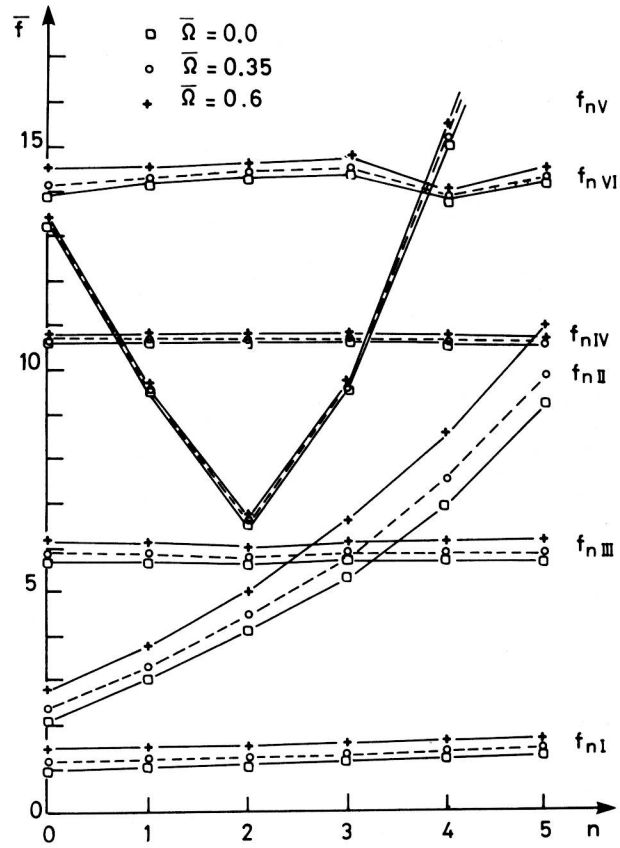

Fig.8 : Turbine stage frequencies versus nodal diameters.

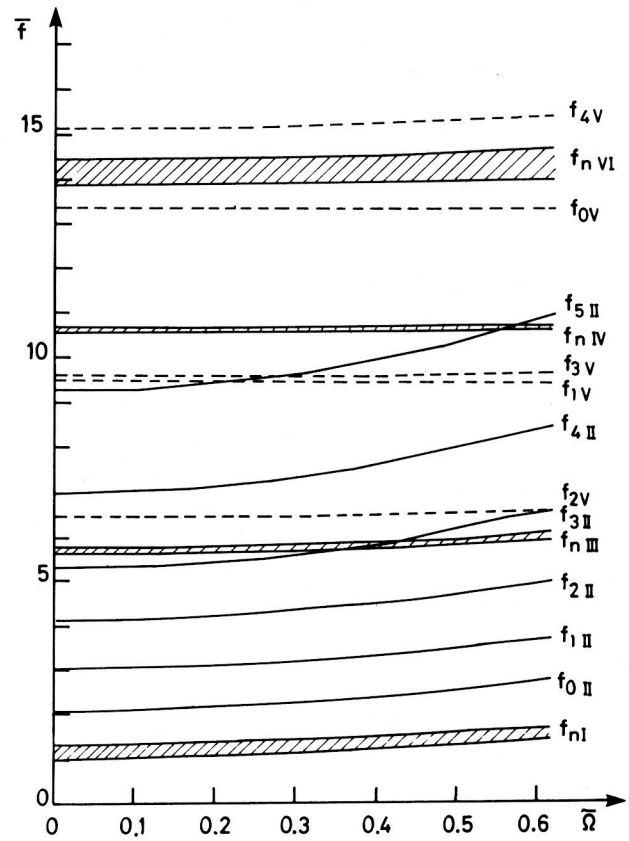

Fig.9 : Turbine stage frequencies versus speed of rotation.

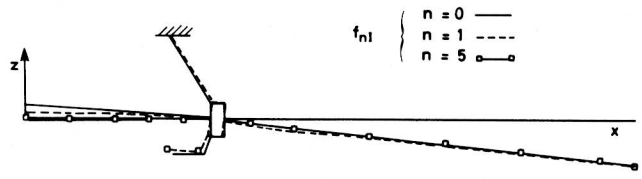

Fig.10 : Mode shapes of f_{nI} for various nodal diameters.

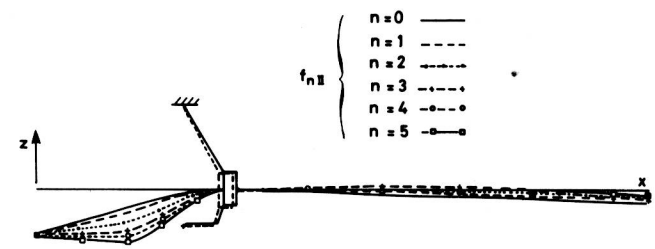

Fig.11 : Mode shapes of family f_{nII}.

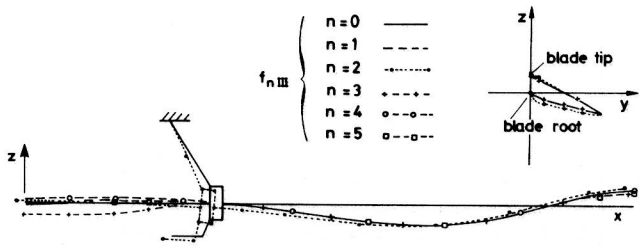

Fig.12 : Mode shapes of family f_{nIII}.

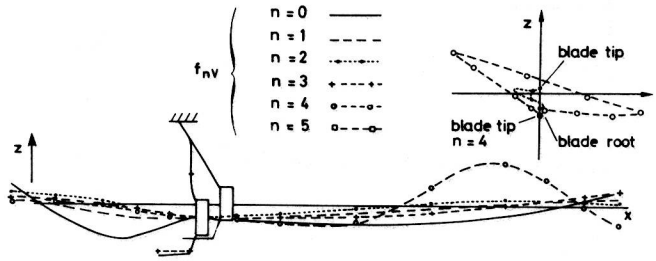

Fig.13 : Mode shapes of family f_{nV}.

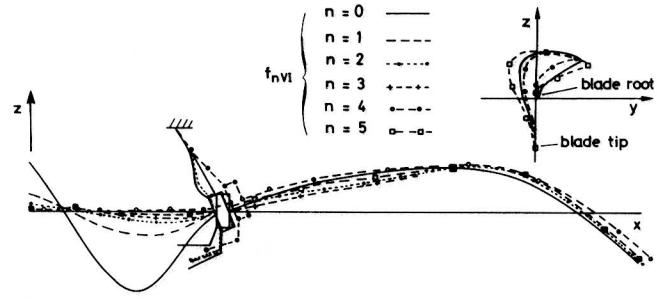

Fig.14 : Mode shapes of family f_{nVI}.

f_{1III}, ..., f_{5II}) ; the associated frequencies increase more than 20 % in the range of Ω studied.

Family f_{nIII}, fig.12 is mainly a blade vibration mode. Its frequencies tend to the first chordwise bending frequency of the clamped blade when the number of nodal diameters increases. The axisymmetric part of the stage undergoes small amplitude of vibration, except for n = 2 and n = 3 which respectively shows large motion for the disc-rim and for the disc. Rotation effect results in a frequency increase of about 8 %.

Family f_{nIV} mode shapes show mostly torsion vibration of the blade with a standing disc. When n increases, the frequency tends to that of the first torsion mode of the clamped blade. It can be seen in fig.9 that the rotation speed Ω has negligible effect, namely 1.5 % for all values of n.

Family f_{nV}, presented in fig.13, shows a disc-rim vibration with strong coupled second bending-torsion motion of the blade and, when n increases, a frequency tending to the second torsion mode of the clamped blade. Except for n = 2, for which frequency increases bout 3.5 %, the rotating effects are negligible.

Family f_{nVI}, fig.14, is a highly coupled vibration mode with important motion of the disc and rim, especially for n = 1 and 4. The blade vibrates on a coupled bending-torsion mode and the frequency tends to the second bending mode of the clamped blade. For this last family, the rotating effects result in a rather small increase of the frequencies (2.5 % for n = 1 to 5 and 5 % for n = 0).

At last, examination of fig.8 and 9 shows clearly that the disc influence is low for the families f_{nI}, f_{nIII}, f_{nIV} and f_{nVI}, and on the contrary is significant for the families f_{nII} and f_{nV}. It can also be noted that the families f_{nI}, f_{nII} and, in some degree f_{nIII}, are affected by the centrifugal effects.

CONCLUSION

The method presented in this paper is well suited for predicting the vibration analysis of any rotating bladed axisymmetric structures with axisymmetric behaviour. The results obtained for the low pressure turbine stage show that an adequate model of such structures must consider all the coupling effects due to the blade and disc geometry along with those due to the rotating effects.

ACKNOWLEDGEMENT

This work was performed as part of numerous studies made during the last ten years in the "Laboratoire de Mécanique des Structures de l'I.N.S.A. de Lyon" on rotating parts of turbomachines and jet engines. The authors are deeply indepted to S.N.E.C.M.A. (Société Nationale d'Etude et de Construction de Moteurs d'Aviation) for its support and permission to publish this paper.

REFERENCES

|1| Armstrong, R., Christie, P.I., Hague, W.M., "Natural frequencies of bladed discs", Proceedings, Institution of Mechanical Engineers, vol.180, Part 1, 1965, pp.110-123.

|2| Ewins, D., "Vibration characteristics of bladed disc assemblies", Journal of Mechanical Engineering Sciences, vol.15, n°3, 1973, pp.165-186.

|3| Ewins, D., Cottney, D.J., "On predicting the natural frequencies of shrouded bladed discs", A.S.M.E. Paper no 75-DET-113, september 1975.

|4| Cottney, D.J., "Natural frequency changes due to shrouding a bladed disc", M. Sc. Thesis, Imperial College, 1971.

|5| Kirkhope, J., Wilson, G.J., "Analysis of coupled blade-disc vibration in axial flow turbines and fans", 12th Structures, Structural Dynamics and Material Conference, Paper no.71.375., 1971.

|6| Thomas, J., Sabuncu, M., "Vibration characteristics of asymmetric cross-section bladed disk under rotation", A.S.M.E. Paper no.79-DET-94, september 1979.

|7| Trompette, P., Lalanne, M., "Frequencies and mode shapes of geometrically axisymmetric structures. Application to a jet engine". Shock and Vibration Bulletin, vol.46, part 5, august 1976, pp.117-122.

|8| Bushnell, D., "Stress, stability and vibration of complex branched shells of revolution", Analysis and User's Manual of Bosor IV.

|9| Rao, J.S., "Natural frequencies of turbine blading-a survey", Shock and Vibration Digest, vol.5, no.10, 1973, pp.3-16.

|10| Rao, J.S., "Turbine blading excitation and vibration". Shock and Vibration Digest, vol.9, no.3, 1977, pp.15-22.

|11| Rao, J.S., "Turbomachine blade vibration", Shock and Vibration Digest, vol.12, no.2, 1980, pp.19-26.

|12| Leissa, A.W., "Vibrations of turbine engine blades by shell analysis", Shock and Vibration Digest, vol.12, no.11, 1980, pp.3-10.

|13| Leissa, A.W., "Vibrational aspects of rotating turbomachinery blades", Applied Mechanics Reviews, vol.34, no.5, 1981, pp.629-635.

|14| Mead, D.J., "A general theory of harmonic wave propagation in linear periodic systems with multiple coupling", Journal of Sound and Vibration, vol.27, no.2, 1973, pp.235-260.

|15| Orris, R.M., Petyt, M., "A finite element study of harmonic wave propagation in periodic structures", Journal of Sound and Vibration, vol.33, no.2, 1974, pp.223-236.

|16| Henry, R., Ferraris, G., "Substructuring and wave propagation : an efficient technique for impeller dynamic analysis", 28th International Gas Turbine Conference, A.S.M.E. Paper no.83.GT.150, March 1983. (To be published in the Journal of Eng. for Power).

|17| Ferraris, G., "Prévision du comportement dynamique des ensembles disque-aubes", Thèse 3ème Cycle, Université Lyon I, february 1982.

|18| Henry, R., "Contribution à l'étude dynamique des machines tournantes", Thèse de Doctorat d'Etat, Université Lyon I, october 1981.

|19| Novozhilov, "Thin shell theory", Walter Noordhoff, 1970.

|20| Saada, A.S., "Elasticity theory and applications", Pergamon Press, 1974.

|21| Rao, J.S., "Turbine blade vibration-continuous system analysis using beam theory", Course, Institut National des Sciences Appliquées de Lyon, Département G.M.D., april 1980.

|22| Montoya, J., "Coupled bending and torsional vibrations in a twisted rotating blade", The Brown Boveri Review, vol.53, n°3, march 1966, pp.216-230.

|23| Leissa, A., "Vibration of plates", N.A.S.A., report, SP 160, 1969, pp.19-30.

|24| Ferraris, G., Henry, R., Gaertner, R., "Détermination des caractéristiques des sections droites quelconques de s poutres. Application aux aubes de turbo-machines" 6ème Congrès Français de Mécanique, Lyon, sept.1983.

APPENDIX

FINITE ELEMENT CHARACTERISTIC GENERALIZED MATRICES

The reference coordinate system is which integration is performed is located at the centroid of the section, thus integrals such as $\iint_S \xi \, dS$ or $\iint_S \eta \, dS$ cancel and are not reported.

Matrix A, equation (20). Noting $A_{ij} = A(I,J)$ and L length of the element yields.

$$A_{11} = A_{32} = A_{46} = A_{73} = -A_{85} = A_{11.4} = 1$$

$$A_{27} = -A_{21} = -A_{5.12} = -0.5\, A_{56} = 0.5\, A_{95} = A_{9.11} = -A_{12.4} = A_{12.10} = 1/L \qquad (A.1.)$$

$$A_{66} = A_{6.12} = -A_{11.5} = -A_{11.11} = 1/L^2$$

$$A_{58} = -A_{52} = -A_{93} = A_{99} = 3/L^2$$

$$A_{62} = -A_{68} = A_{11.3} = -A_{11.9} = 2L^3$$

Generalized stiffness matrix, equation (27).

$$|k_e+k_g| = \iint_S dS \begin{array}{|c|c|c|c|c|c|} \hline E+\sigma_0 & 0 & 0 & 0 & 0 & Ek\theta' \\ \hline & \sigma_0(1+\eta^2\theta'^2) & -\sigma_0\xi\eta\theta'^2 & -\sigma_0\xi\eta\theta' & -\sigma_0\eta^2\theta' & 0 \\ \hline & & \sigma_0(1+\xi^2\theta'^2) & \sigma_0\xi^2\theta' & \sigma_0\xi\eta\theta' & 0 \\ \hline & & & \xi^2(E+\sigma_0) & \xi\eta(E+\sigma_0) & -Ek\xi\theta'-\sigma_0\eta_t x \\ \hline & \text{Symmetry} & & & \eta^2(E+\sigma_0) & -Ek\eta\theta'+\sigma_0\xi_t x \\ \hline & & & & & Ek^2\theta'^2+\sigma_0 h+\left|d/dS\,(GJ_T)\right|^{*} \\ \hline \end{array} \qquad (A.2.)$$

k and h are given in Eq.(15) and σ_0 initial stress is calculated in solving Eq.(40).

(*) Means that $|\ |$ is still integrated so as $\iint_S \frac{d}{dS} |GJ_T| \, dS$ gives GJ_T after integration.

Generalized mass matrix, equation (34).

$$|m_e| = \iint_S dS. \begin{array}{|c|c|c|c|c|c|} \hline 1 & 0 & 0 & 0 & 0 & 0 \\ \hline & 1 & 0 & 0 & 0 & \eta_t \\ \hline & & 1 & 0 & 0 & -\xi_t \\ \hline & & & \xi^2 & \xi\eta & 0 \\ \hline & & & & \eta^2 & 0 \\ \hline & & \text{Sym.} & & & \xi^2+\eta^2+\xi_t{}^2+\eta_t{}^2 \\ \hline \end{array} \quad \text{(A.3.)}$$

Generalized centrifugal stiffness matrix, equation (35).

Remembering that Ω_1, Ω_2, Ω_3 are the components of the angular velocity vector $\vec{\Omega}$ expressed in the rotating local coordinate system of the element, fig.6

$$|k_c| = \iint_S dS. \begin{array}{|c|c|c|c|c|c|} \hline \Omega_2{}^2+\Omega_3{}^2 & -\Omega_1\Omega_2 & -\Omega_1\Omega_3 & 0 & 0 & \Omega_1(\xi_t\Omega_3-\eta_t\Omega_2) \\ \hline & G & F & 0 & 0 & \eta_t(\Omega_1{}^2+\Omega_3{}^2)+\xi_t\Omega_2\Omega_3 \\ \hline & & E & 0 & 0 & -\xi_t(\Omega_1{}^2+\Omega_2{}^2)-\eta_t\Omega_2\Omega_3 \\ \hline & & & D & C & \Omega_1(\xi^2\Omega_3-\xi\eta\Omega_2) \\ \hline & \text{Sym.} & & & B & \Omega_1(\xi\eta\Omega_3-\eta^2\Omega_2) \\ \hline & & & & & A \\ \hline \end{array} \quad \text{(A.4.)}$$

$A = (\xi^2+\xi_t{}^2)(\Omega_1{}^2+\Omega_2{}^2)+(\eta^2+\eta_t{}^2)(\Omega_1{}^2+\Omega_3{}^2)+2\Omega_2\Omega_3(\xi\eta+\xi_t\eta_t)$

$B = \eta^2(\Omega_2{}^2+\Omega_3{}^2)$

$C = \xi\eta(\Omega_2{}^2+\Omega_3{}^2)$

$D = \xi^2(\Omega_2{}^2+\Omega_3{}^2)$

$E = \Omega_1{}^2+\Omega_2{}^2$

$F = -\Omega_2\Omega_3$

$G = \Omega_1{}^2+\Omega_3{}^2$

Generalized centrifugal force vector, equation (36).

Remembering that x_I, ξ_I, η_I are the components of the vector $\vec{OG}_I$ (node N_I) expressed in the local system $R_i(Gx\xi\eta)$, fig.6.

$$\{f_c\} = \iint_S dS. \begin{array}{|l|} \hline (\Omega_2{}^2+\Omega_3{}^2)(x+x_I)-\Omega_1\Omega_3\eta_I-\Omega_2\Omega_3\eta_I \\ \hline (\Omega_3{}^2+\Omega_1{}^2)\xi_I-\Omega_2\Omega_1(x+x_I)-\Omega_2\Omega_3\eta_I \\ \hline (\Omega_1{}^2+\Omega_2{}^2)\eta_I-\Omega_2\Omega_3\xi_I-\Omega_3\Omega_1(x+x_I) \\ \hline \Omega_1\Omega_2\xi^2+\Omega_1\Omega_3\xi\eta \\ \hline \Omega_1\Omega_3\eta^2+\Omega_1\Omega_2\xi\eta \\ \hline (\Omega_1{}^2+\Omega_3{}^2)\xi_I\eta_t-(\Omega_1{}^2+\Omega_2{}^2)\eta_I\xi_t+(\Omega_2{}^2-\Omega_3{}^2)\xi\eta \\ +(\Omega_1\Omega_3\xi_t-\Omega_1\Omega_2\eta_t)(x+x_I) \\ +\Omega_2\Omega_3(\eta^2-\xi^2+\xi_I\xi_t-\eta_I\eta_t) \\ \hline \end{array} \quad \text{(A.5.)}$$

FREE AND FORCED VIBRATION OF TURBINE BLADES

J. S. Rao, Professor and Head Mechanical Engineering
Indian Institute of Technology
New Delhi, India

H. M. Jadvani, Assistant Professor of Mechanical Engineering
Regional Engineering College
Surat, India

ABSTRACT

The kinetic and strain energy expressions for a tapered twisted aerofoil cross-section blade mounted at a stagger angle on a rotating disk are obtained using beam theory neglecting higher order effects such as shear deformation, rotary inertia, coriolis forces. Equations of Lagrange are used to derive equations of motion and set up the eigenvalue problem to obtain the coupled bending-bending-torsion mode frequencies. Assuming proportional viscous damping the expression for energy dissipated in the rotating blade is derived. The virtual work due to nozzle passing excitation is also set up and the equations of motion for forced vibrations of a blade are derived. These equations are solved by modal analysis. A general computer program is developed to determine the response of the blade and the results obtained are discussed.

NOMENCLATURE

A	Area of cross-section
A_i	Polynomial coefficients of function $A(z)$
a, b	Coefficients in trigonometric series of forcing functions
C	Torsional stiffness
$[C]$	Damping matrix
c_v	Proportional damping coefficient
E	Modulus of elasticity
$\bar{e}$	Unit vector
f_i, F_i	Shape functions
F_x, F_y	Forcing functions
G	Modulus of rigidity
I_{xx}, I_{yy}	Second moment of area about centroidal axes
I_{xy}	Product moment of area about centroidal axes
I_{xx}, I_{yy}	Principal second moments of area
I_{cf}, I_{cg}	Moments of inertia per unit length about centre of flexure and centre of gravity respectively
I_1, I_2	See equation (22)
I_{xi}, I_{yi}	Polynomial coefficients of functions I_x, I_y
$[K]$	Stiffness matrix
L	Blade length
$[M], M$	Mass matrix, moment
m	Harmonic number
n	Number of terms in assumed solution
n_s	Number of nozzles
$\{Q\}$	Forcing vector
q	Time function
R	Disc radius
$\bar{r}$	Position vector
r_x, r_y	Coordinates of centre of flexure from centroid
T	Kinetic energy
t	time
U	Displacement vector
u	Displacement in axial direction due to centrifugal force
u_x, u_y, u_z	Displacement components
V	Potential energy
v	Velocity
W_d	Energy dissipated due to proportional viscous damping
W_f	Work done by external forces

x, y	Bending displacements in x and y directions
x_1, y_1	Bending displacements in x_1 and y_1 directions
xx, yy	coordinate axes through centre of flexure
x_1x_1, y_1y_1	coordinate axes through centroid.
z	Distance measured along length of the blade
Z	z/L
ρ	Mass density
ω	Angular velocity of Disc
ω_k	Natural frequency in kth mode
θ	Torsional deflection
ϕ	Stagger angle
ν	Nozzle passing frequency $= n_s\omega$
δ	Virtual parameter
η	Generalised coordinate
$\eta\zeta$	Tangential-axial coordinate system
ζ	Modal damping
$\bar{}$	Denotes either a vector or sub-matrix, thus, $\bar{x}, \bar{\bar{x}}$
$'$	Denotes differentiation with respect to z , thus, y'
$\dot{}$	Denotes differentiation with respect to t , thus, $\dot{y}$
$\cdot$	Denotes coordinate quantity, thus, $\dot{x}$

INTRODUCTION

Blades constitute the heart of the turbomachine and as such they have been subjected to a very intensive theoretical and experimental study during the last two decades mainly due to the advent of high speed machines. It is known from investigations that the failure of turbine blading is normally due to fatigue and it occurs when vibrations take place at or near resonant conditions. In earlier designs fatigue failures were avoided by tuning the blade to operate away from the natural frequencies. However, a typical modern machine may have 3 or 4 rotors, each rotor having several stages and the turbine altogether may have thousands of blades of different characteristics. Here in such machines, it is not always possible to avoid resonance conditions in some stages. Under these conditions the designer should estimate the blade response and dynamic stresses at resonance conditions. With the help of this information, a blade can be designed for the required life to withstand the dynamic stresses.

Generally the blades in the low pressure stages of a turbine are quite long and flexible, due to specific volume of the fluid being too large in these stages. The blades are tapered and twisted and have airfoil cross-section to provide high lift to drag ratio. Free and forced vibration of such blades are considered in this paper. Extensive literature is available in this area; as many as 450 papers were reviewed (1-4) in a series of articles in the last decade. Three other reviews on allied topics appeared in the last three years (5-7). Some of the recent works on blade vibration include the following: Pre-twisted rotating blades, Jadvani and Rao (8); Irretier and Schmidt (9) on mistuned blades, Ewins (10) on bladed disks with packeting; Muszynska and Jones (11) on response of mistuned bladed disk system. Sogliero and Srinivasan (12) used statistical procedure to estimate fatigue life of mistuned rotor blades due to stationary Gaussian white noise process excitation. Partington (13) described a vibration design method for pinned root control stage blades. The instabilities due to harmonic variation with time of the precessional rate due to whirling and other causes were discussed by Sisto et al (14).

CHARACTERIZATION OF BLADE RESPONSE

The response of the blade can be described in terms of bending displacements $x(z,t)$, $y(z,t)$ of the point O, which is center of flexure of the cross-section of the blade shown in figure 1 and torsional displacement $\theta(z,t)$ with respect to the same point. A particle initially at Point P with coordinates x, y in Oxy axis system, moves to point P_1 under the influence of angle of rotation θ, resulting in an inward displacement $y\theta$, and outward displacement $x\theta$ in x and y directions respectively. This point P further moves from P_1 to P_2 by $x(z,t)$ and then vertically to position P' by $y(z,t)$ under the influence of bending displacements. Hence the x and y displacements u_x and u_y of the particle P can be written as

$$u_x = x - y\theta \qquad (1)$$
$$u_y = y + x\theta$$

In figure 1 an axes system x_1y_1 through the centroid G is also used to describe the bending displacements, which identifies the stagger angle ϕ with respect to the ζ axis in the plane of rotation of the disk as shown in figure 2. In figure 2 the blade is occupying a position Γ, for the instance shown in fixed axis system CMN. xy and x_1y_1 axes in figure 1 are displaced by r_x in x direction and r_y in y direction respectively. The displacements in equation (1) can therefore be written as :

$$u_x = (x + r_y\theta) - y_1\theta = x_1 - y_1\theta$$
$$u_y = (y + r_x\theta) + x_1\theta = y_1 + x_1\theta \qquad (2)$$

In the above equation x_1 and y_1 denote the bending displacements of the centroid of the cross-section and x and y denote the bending displacement of center of flexure O.

The point P described before, moving from P to P_1, P_1 to P_2 and P_2 to P', further moves longitudinally in z direction by $u(z,t)$ under the action of centrifugal forces. It has a further